RSC Advances

ROYAL SOCIETY
OF CHEMISTRY

www.rsc.org/advances

Fracture damage of nanowire Lithium-ion battery electrode affected by diffusion-induced stress and bending -during lithiation

Bingbing Chen[a] , Jianqiu Zhou[a,b,*], Xuming Pang[a], Pengfei Wei[a], Yunbo Wu[a], Kunjun Deng[a]

[a]Department of Mechanical Engineering, Nanjing University of Technology, Nanjing, Jiangsu Province 210009, China

[b]Department of Mechanical Engineering, Wuhan Institute of Technology, Wuhan, Hubei Province 430070, China

*Corresponding author.Tel.:+86-25-83588706; Fax: +86-25-83374190.

E-Mail addresses: zhouj@njut.edu.cn, chenbingbing1990@126.com

Abstract

The Lithium-ion battery electrode materials generally experience the significant volume changes during lithium diffusion in the charging and discharging. It leads to diffusion-induced stress and defect nucleation. By analyzing the stress, bending - associated with lithiation, we find that the size reduction of electrode can avoid the phenomenon of volume changes. In this work, we built a relationship among the stress, bending, strain energy and size of the electrode. And the fracture energy of the electrode materials, which can be evaluated by the strain energy further, has been derived to optimize the electrode size to maximize the battery life. Finally, the critical electrode size determination method is proposed.

1. Introduction

In recent years, many investigations[1-3] have been performed to study the Lithium-ion battery cells as secondary battery systems because of high energy density, high efficiency of charge-discharge, high operating voltages compared to conventional cells. It has been recognized that development of battery electrodes materials will be a critical factor for large capacity energy storage, So many materials have received attention such as Si, Sn, MnO_2, Sb, Mg, Bi.[4] For example, It had been found that use of tin oxide nanowires as electrodes materials can increase about twice the discharge capacity than the lithium-ion rechargeable batteries using graphite carbon.[5] SnO_2 is one of the most promising anode materials to replace the carbonous anodes used in Li-ion batteries, because of having a theoretical capacity of $781mAhg^{-1}$ and reversible capacity exceeding $500mAhg^{-1}$.[6-9] However, there are very large stresses owing to volume changes (up to 260%)[10-12] during Li insertion/extraction processes in Li-ion battery electrode, it will lead to serious electrodes irreversible capacity and poor cyclability.[13] Many experiments demonstrate[14,15] that size reduction of nanowires is one of the effective strategies to resist the fracture.

So far, some previous studies have analyzed the stresses induced by the diffusion of Li^+. Huggins et al.[16] have used Griffith criterion to exposit fracture in a one-dimensional model and Aifantis et al.[17] used Griffith's criteria to estimate critical crack size under which the crack will not propagate for nanostructured in Li-ion batteries. Recently, the dislocations about the diffusion have been researched. Wei et al.[18] analyzed the effect of the dislocation mechanics on diffusion induced

stresses within a spherical article. To avoid pre-existing crack, Gao et al.[19,20] developed a cohesive model of crack nucleation and suggested a critical characteristic dimension to avoid the fracture. Zhao et al.[21] used strain energy release rate to estimate the crack propagation and developed a fracture criterion in the electrode particles. Despite these contributions, the diffusion and damage process still keeps not well understood.

In the paper, we will constuct a model to explain the fracture behavior during lithiation and develop a method to predict the critical electrode size. The size reduction of nanowires has been reached a good agreement on the avoidance the fracture.[14-22] Following this, we continue to do further work on how to prevent the fracture behaviors in the electrode materials. The stress and bending deformation will be first obtained in the Li-ion batteries electrodes by finite elasticity-plasticity theory.[18-21] Then, the equations to describe the strain energy for the nanowires (NW) containing preexisting cracks will be proposed. These strain energy will be used to derive fracture energy and estimate the critical electrode size.

2. Stress in a cylindrical electrode

According to the theory of lithium battery, we can know that lithium ions will diffuse out of the anode when the battery discharges. The material of electrode is assumed as an isotropic linear elastic solid and the mechanics behavior is changed from elastic to elastic-perfectly plastic. Simultaneously, we assume the lithium transport is purely diffusive in active material particles. In this paper, The schematic illustration of stress in a cylindrical electrode at the surface current density

during galvanostatic as shown in the Fig.1. There are diffusion process equations to deal with the diffusive flow of lithium by[23]

$$\frac{\partial c}{\partial t} = \frac{1}{r}\frac{\partial}{\partial r}\left(rD\ \frac{\partial c}{\partial r}\right)$$

(1)

where D is the diffusion coefficient as constant, c is the molar concentration of solute. The transformation strain ε_t owing to insertion of solute atoms connect with the partial molar volume Ω and the concentration c.

$$\varepsilon_t = \frac{\Omega C}{3}$$

(2)

We assume that the surface lithium ion concentration is C_R and the initial lithium ion concentration is C_0 in the electrode, so the initial and boundary conditions are given by

$C(r,0) = C_0,$ for $0 \le r \le R$ (3)

$C(R,0) = C_R,$ for r=R (4)

We consider stress caused by Li^+ diffusion within a nanowires of radius R. The stress–stain relationships, expressed in the spherical coordinate system using the analogy between thermal and DIS.[18-20,24-26] So we can know that general relations for the stresses and strain in a cylinder.

$$\varepsilon_r - \varepsilon_t = \frac{1}{E}\left(\sigma_r - \mu(\sigma_\theta + \sigma_z)\right)$$

(5)

$$\varepsilon_\theta - \varepsilon_t = \frac{1}{E}\left[\sigma_\theta - \mu(\sigma_r + \sigma_z)\right]$$

(6)

Where μ is the Poisson ratio of the material and E is the Young's modulus. And the diffusion process along the r-direction of the electrode. The equation for static

mechanical equilibrium and kinematic relations in the cylindrical of the NW is given by[26]

$$\varepsilon_r = \frac{du}{dr}, \varepsilon_\theta = \frac{du}{r} \tag{7}$$

$$\frac{d\sigma_r}{dr} = \frac{\sigma_\theta - \sigma_r}{r} \tag{8}$$

In the plane strain conditions, the the radial, tangential and axial stresses that satisfies the boundary condition in the cylinder by the dynamics can be given by:

$$\sigma(r,t) = \frac{E}{1-\mu}\left[\frac{2}{R^2}\int_0^R \frac{\Omega C(r)}{3}rdr - \int_0^r \frac{\Omega C(r)}{3r^2}\right] \tag{9}$$

$$\sigma(\theta,t) = \frac{2E}{1-\mu}\left[\frac{2}{R^2}\int_0^R \frac{\Omega C(r)}{3}rdr + \int_0^r \frac{\Omega C(r)}{3r^2} - \frac{C(r)}{3}\right] \tag{10}$$

$$\sigma(z,t) = \frac{E\Omega}{1-\mu}\left(\frac{2}{3R^2}\int_0^R Crdr - \frac{C}{3}\right) \tag{11}$$

Hence, diffusion induced stresses at any location of electrode and time without considering the bending effect near the ends can be obtained if the composition

3. Bending stress in the electrode.

profile is known.

Understanding the diffusion-induced stress in the cylinder electrodes, there is no bending at points at a large distance from the free ends. So the stresses can be calculated from Eqs.(9)-(11). However, there are some bending near the end,[34] which will generate chemical stresses in the elastic cylinder. For the non-uniform distribution of the solute atoms, we will consider the bending deformation of the cylinder because of the diffusion-induced stress in the cylinder electrodes. According

the Euler-Bernoulli beam assumption through the incremental deformation theory, the bending moments can be expressed as

$$M = \int_0^R \sigma(r-R)rdr = \frac{E\Omega}{3(1-\mu)}\left(\frac{R}{3}\int_0^R Crdr - C\right)$$ (12)

So the bending moments introduce the stress can be found as

$$\sigma(r,t)^1 = -\frac{M}{I}(r-R) = -\frac{4E\Omega}{R^3(1-\mu)}(r-R)\left(\frac{R}{3}\int_0^R Crdr - C\right)$$ (13)

To prevent the cross sections of the strip from distortion during the diffusion induced bending, the moments applied to the strip are μM ,

$$\sigma(\theta,t)^1 = -\frac{\mu M}{I}(r-R) = -\frac{4\mu E\Omega}{R^3(1-\mu)}(r-R)\left(\frac{R}{3}\int_0^R Crdr - C\right)$$ (14)

Thus, the stress can be approximately as near the ends

$$\sigma(r,t)^r = \frac{E}{1-\mu}\left[\frac{2}{R^2}\int_0^R \frac{\Omega C(r)}{3}rdr - \int_0^r \frac{\Omega C(r)}{3r^2}\right] + \sigma(r,t)^1$$ (15)

$$\sigma(\theta,t)^\theta = \frac{2E}{1-\mu}\left[\frac{2}{R^2}\int_0^R \frac{\Omega C(r)}{3}rdr + \int_0^r \frac{\Omega C(r)}{3r^2} - \frac{C(r)}{3}\right] + \sigma(\theta,t)^1$$

(16)To comprehend the stress due to the diffusion, the boundary conditions under galvanostatic can be found as

$$D\frac{\partial c}{\partial r}\bigg|_{r=0} = 0$$ (17)

$$-D\frac{\partial c}{\partial r}\bigg|_{r=R} = -J_n$$ (18)

Where J_n is surface current density. During the charging, The J_n can be obtained as

$$J_n = J_0(1 - C_R/C_{max})$$ (19)

7

where J_o is the charging rate. Eq. (19) is a linearized form of the Butler–Volmer Equation.[28] And the solute concentration during lithiation can be expressed by[13]

$$\frac{C - C_0}{C_1 - C_0} = 1 + 2\sum_{n=1}^{\infty} \frac{(-1)^n}{n\pi(r/R)} \sin\left(\frac{n\pi r}{R}\right) e^{-n^2\pi^2 Dt/R^2}$$

(20)

During charging, the Li^+ will be extracted from the anode and inserted to the cathode. It will be the opposite in the discharging. There are only discussing the situation of the lithiation. So the diffusion-induced stress and bending stress can be   calculated by the the stress solution and the concentration solution in the plane strain during lithiation.

The concentration profiles can be depicted using the Eq. (18) in the Fig.2. From Fig.2, we can see that the concentration continuously rises with charge time   Then, concentration profile will get a steady state after some charge time during insertion. Without considering bending moment, thediffusion induced   stresses will be shown in Fig.3 during insertion. The radial stress is tensile and the maximum radial stress occurs at the center in the cylindrical in the Fig.3(a). In addition, the radial stress will be deceases with increasing the concentration. From Figs.2-3(a), we see the maximum stress occurs at the center when the time after the solute reaches the center of the cylindrical. The tangential stress is compressive near the surface and tensile near the center of the cylindrical in the Fig.3(b). In addition, the maximum tangential stress will be happen at the surface of the cylindrical. Fig.3(c) shows that the axial stress is tensile near the center and compressive near the surface of the electrode. It is

worth noting that the axial stress get a stabilize condition and the maximum tensile stress occurs at the center. To indicating the bending impact, the bending stress will be shown in the Fig.4. The variation of the bending stress with the diffusion time and different diameters will be shown near the ends. What's more, the bending stress of the cylindrical electrode is always at compressive state under the potentiostatic operation. In the paper, radial stress will be plotted in the Fig.5 at the same charging rate and the short dots lines represents the axial stress with considering the bending deformation. Form Figs.4-5, we can see the bending deformation effect can't be negligent . For insertion, the axial stress are plotted with different size of electrode at dimensionless time T=0.5   in the Fig.6. It is obvious that the maximum stress at the center will increase with the rising of the diameter . From Figs.2 -6, it is clear that the size of the electrode are very important to the cylindrical electrode.

4. Strain energy and Fracture in the cylindrical electrode

To estimate the fracture resistance, we assume that cracks may exist in the NW of the battery. Ref. [29] shows the strain energy in the particles. For nanoscale wires, The strain energy contains the bulk energy and   bending energy. According to the theory of the linear incremental constitutive relation[30], we suppose the incremental deformation is infinitesimal. When small deformations are assumed, the strain energy release rates will be linearly with the size. we can calculate the strain energy density accumulated as a result of the deformation for the isotropically deformed cylinder

$$e(r) = \frac{(\sigma_\theta + \sigma_r + \sigma_z)^2 - 2\mu(\sigma_r\sigma_\theta + \sigma\theta\sigma_z + \sigma_r\sigma_z)}{2E}$$

(21)Strain energy which is stored in the electrode because of the elastic deformation

and the section strain energy can be obtained by integrating the strain energy density

over the entire volume of the NW

$$E_\gamma = 2\pi \int_0^R e(r)rdr$$ (22)

Because of the bending moment effects, the energy due to bending stress should be

considered. The the schematic illustration of bending near the ends will be

specialized in the Fig.7. The bending of the cylinder electrode can be calculated by

$$D\frac{d^4w}{dr} = -\frac{Ehw}{R^2}$$ (23)

The solution of the Eq.(23) with the moment applied to the end is

$$w = -\frac{M}{2\beta^2\partial}e^{-\beta z}(\cos\beta z - \sin\beta z)$$ (24)

Where the $\beta = \left(\frac{3(1-\mu^2)}{R^2r^2}\right)^{1/4}$ and the $\partial = Er^3/12(1-\mu^2)$ is the flexural rigidity in

the axial direction. So the largest deflection,which occurs at the z become zero, will

be expressed as

$$w_{max} = -\frac{E\Omega}{6(1-\mu)\beta^2\partial}\left(\frac{R}{3}\int_0^R Crdr - C\right)$$ (25)

This condition could be similar to the linear stress–strain relations and the energy

could be calculated as

$$E_\eta = 2\pi\int_0^R \sigma(r,t)^1 w_{max}rdr \quad (26)$$

So the total strain energy could be written as

$$E_T = E_\gamma + E_\eta = 2\pi \int_0^R \left(\frac{\sigma_z^2}{E} + \sigma_\chi w \right) r dr \tag{27}$$

From above we can define strain energy with dimensionless form as $\hat{E}_T = E_T / \pi E (\Omega C / 3(1-\mu))^2$. Fig.8 shows that variation of strain energy in the axial loading conditions without considering the bending deformation. The difference in the strain energy profiles in the four cases owes to the different the size of NW From this, strain energy increases initially and reaches a peak values with the charge time. In addition, the strain energy is increasing with the size of the electrodes and increasing charging time. When the bending deformation considered, the stain energy will be plotted at the 200nm cylindrical electrode and the short dots lines represents the strain energy with considering the bending moment in the Fig.9. From the Fig.9, the bending deformation has a great impact in the electrode about energy. Significantly, we can see that the strain energy is related to the charge time and size of NW. So the strain energy should take the form by the dimensional considerations

$$E_T = KJ_o \Omega R \Big/ \pi D \left(\frac{\Omega C}{3(1-\mu)} \right)^2$$

(28)

Where K may be determined by the elastic boundary-value problem and it is affiliated with the length of the crack and time. In these, the stain energy reaches the maxi-mum value E_T for a crack. Let Γ be the fracture energy of the electrode. When the maximum stain energy locates below the fracture energy of the electrode, crack nucleation will not happen. And this has been schematically shown in the Fig.10. No fracture will be occur in the area where $E_T < \Gamma$.

Based on above, we can propose a critical NW size as follows.

$$L = K\pi \left(\frac{\Omega C_{max}}{3(1-\mu)} \right)^2 \frac{D}{J_o \Omega} \frac{\Gamma}{E} \tag{29}$$

It is obvious that the critical size relies on the charging rate. And we plot the critical size related to the J_o in the Fig.11. If the charging rate is known, the critical size can be figured out the electrode critical size. Many experimental observations [15,31,33] show that the critical size of Si wire electrode is in the range of 220-260nm at the rate of 0.2mVs[-1]. We may predict the critical size using the same experimental data and analysis. The critical size is about 240nm by the Eq.(29) using the parameters in Table1. It agrees with the experimental data [15,31] at the same charging rate.**5. Conclusions**

We have developed a method to evaluate the stress in a cylindrical nanostructured electrode under galvanostatic conditions using a combination of diffusion kinetics and fracture mechanics. To predict the fracture, we analyze the stresses and bending deformation associated with lithiation and use the strain energy to predict the fracture behavior. The strain energy is derived under the bending deformation considered If the maximum strain energy is less than the fracture energy of the material, there is no crack nucleation and propagation. Finally, the critical size was obtained by the fracture energy   and the boundary conditions about plane strain of the nanowire electrodes were considered. The critical size are related to the charging rates, material properties and fracture energy. To illustrate the theory, a numerical example of Si NW is calculated. In this case we can see that the diameters of the Si

NW, which is smaller than 220-260nm will not fail in the lithiation process. The conclusions are in agreement with the experiments. Thus the method in this paper can be used to optimize the size of cylindrical electrode and maximize the battery life.

References

1 F. Hao, X. Gao , D. N. Fang. J. Appl. Phys. 112, 103507 (2012)

2 M. Holzapfel, H. L. Buqa, L. J. Hardwick, M. Hahn, A. Würsig, W. Scheifele, P. Novák, R. Kötz, C. Veit, F. Petrat. Electrochim. Acta 52, 973 (2006)

3 C.de las. Casas, W. Z. Li. J. Power Sources 208, 74 (2012)

4 W.-J. Zhang. J. Power Sources 196, 13 (2011) .

13

5 F.M. Courtel, E.A. Baranova, Y. A-Lebdeh, L.J. Davidson. J. Power Sources 195 ,2355 (2010)

6 L. Yuan, Z.P. Guo, K. Konstantinov, H.K. Liu, S.X. Dou. J. Power Sources 159, 345(2006)

7 H.D. Liu, J. Huang, X.L Li, J. Liu, Y.X Zhang. Ceramics International 38, 5145 (2012)

8 Z.J. Du, S.C. Zhang, T. Jiang, X.M Wu, L. Zhang, H. Fang. J. Power Sources 219,199 (2012)

9 Z.G. Wen, F. Zheng, H.C Yu, Z. Jiang, K.L Liu. Materials Characterization 76,1 (2013)

10 M. Winter, J.O. Besenhard, M.E. Spahr, P. Novak. Advanced Materials 10, 725 (1998)

11 C.L. Lim, B.Yan, L.L Yin, L.K. Zhu. Electrochim. Acta 75, 279（2012)

12 S. Bourderau, T. Brousse, D.M. Schleich. J. Power Sources 81, 233 (1998)

13 B. Laforge, L. Jodin-Levan, Salot. J. Electrochem. Soc. 155, A181 (2008)

14 Y.-T. Cheng, M.W. Verbrugge. J. Appl. Phys104, 083521 (2008)

15 I. Ryu, J.W. Choi, Y. Cui, W. D. Nix. J. Mechanics and Physics of Solids 59 ,1717 (2011)

16 R.A. Huggins, Nix, W.D. Ionics 6, 57 (2000)

17 K.E. Aifantis, S.A. Hackney, J.P. Dempsey. J. Power Sources165,874 (2007)

18P. Wei, J. Zhou and X.Pang, J. Mater. Chem. A, 2013, DOI: 10.1039/C3TA13925E

19 T. K. Bhandakkar, H.J. Gao. J. Mechanics and Physics of Solids 47, 1424 (2010)

20 T.K. Bhandakkar, H.J Gao. J. Mechanics and Physics of Solids 48, 2304(2011)

21 K.J Zhao, M. Pharr, L. Hartle, J.J. Vlassak, Z.G. Suo. J. Appl. Phys, 108, 073517(2012)

22 H. Haftbaradaran, J. Song, W.A. Curtin, H.J. Gao. J. Power Sources196, 361 (2010)

23 J. Crank, The Mathematics of Diffusion. Oxford University Press (1980)

24 S.P. Timoshenko, J.N. Goodier, Theory of Elasticity. McGraw-Hill Book Company (1970)

25 F. Yang. Materials Science and Engineering: A 409 ,153 (2005)

26 X. Zhang, W. Shyy, A.M. Sastry. J. Electrochemical Society 154, A910 (2007)

27 M. E. Gurtin. International Journal of Solids and Structures 14, 431 (1978)

28 C.H. Chen, N. Ding. Solid State Ionics, 180, 222 (2009)

29 Y.-T. Cheng . J. Power Sources 190,453 (2009)

30 M.A. Biot, Mechanics of Incremental Deformations. Wiley, New York（1965）

31 R. Teki, M.K. Datta. Small 5, 2236 (2009)

32 K. Rhodes, N. Dudney, E. Lara-Curzio, C. Daniel. J. Electrochem. Soc. 157, A135 (2010)

33 H. Wu, Y. Cui. Nano Today 7, 414 (2012)

34 Fuqian Yang. Mechanics Research Communications 54, 72 (2013)

Tabe1. Material properties and operating parameters

Parameter	symbol	value
Diffusion coefficient	D	$2 \times 10^{-18} m^2 s^{-1}$ [a]
Youg's modulus of lithiated Si	E	90.13GPa[b]
molar volume of Si	Ω	$1.2052 \times 10^{-5} m^3 mol^{-1}$[a]
Poisson's ratio of Si electrode	μ	0.22[a]
maximum concentration	C_{max}	$2.0152104 \times 10^4 m^3 mol^{-1}$[a]
Fracture energy	Γ	$2 J m^{-2}$ [c]

[a] Ref. 20

[b] Ref. 32

^{c} Ref. 22

Figure captions

Fig 1. Schematic illustration of stress in a cylindrical electrode at the surface current

density during galvanostatic.

Fig 2.

Lithium ion concentration profile in the electrode at different radial locations and

times during insertion.

Fig 3. Profiles of diffusion induced stress during insertion, (a) radial stress during

insertion at the different locations and charging times , (b) tangential stress   at at the

different locations and times. (c) axial stress at the different locations and times. The

stress is normalized as $\hat{\sigma} = 3\sigma(1-\mu)/E\Omega C$.

Fig 4. Profiles of bending stress at the the diffusion time and different diameters near.

The stress is normalized as $\hat{\sigma} = 3\sigma(\theta,t)(1-\mu)/E\Omega C$

Fig 5. Radial stress during insertion for various charging time. The solid line

represents the stress without the bending effect and the short dots line represents the

stress considering the bending effect.Fig 6. Profiles of the axial stress with different

diameters at dimensionless T=0.5

Fig 7. Schematic illustration about the bending effect in a cylindrical electrode.

Fig 8. Profiles of strain energy with different diameters The strain energy varies with

time and increases with the diameters of the electrodes. The strain energy is

normalized as $\hat{E_T} = E_\gamma / \left[\pi R^2 E \left(\frac{\Omega C}{3(1-\mu)} \right)^2 \right]$ Fig 9. Strain energy at the 200nm

cylindrical electrode. The solid line represents the energy without the bending effect

and the short dots line represents the energy considering the bending effect. The

strain energy is normalized as $\hat{E_T} = E_T / \left[\pi R^2 E \left(\frac{\Omega C}{3(1-\mu)} \right)^2 \right]$

Fig 10. Sketched schematically concept for the criteria to avert fracture for the

electrode

Fig 11. Critical electrode size at different fracture energy with different charging

rates.
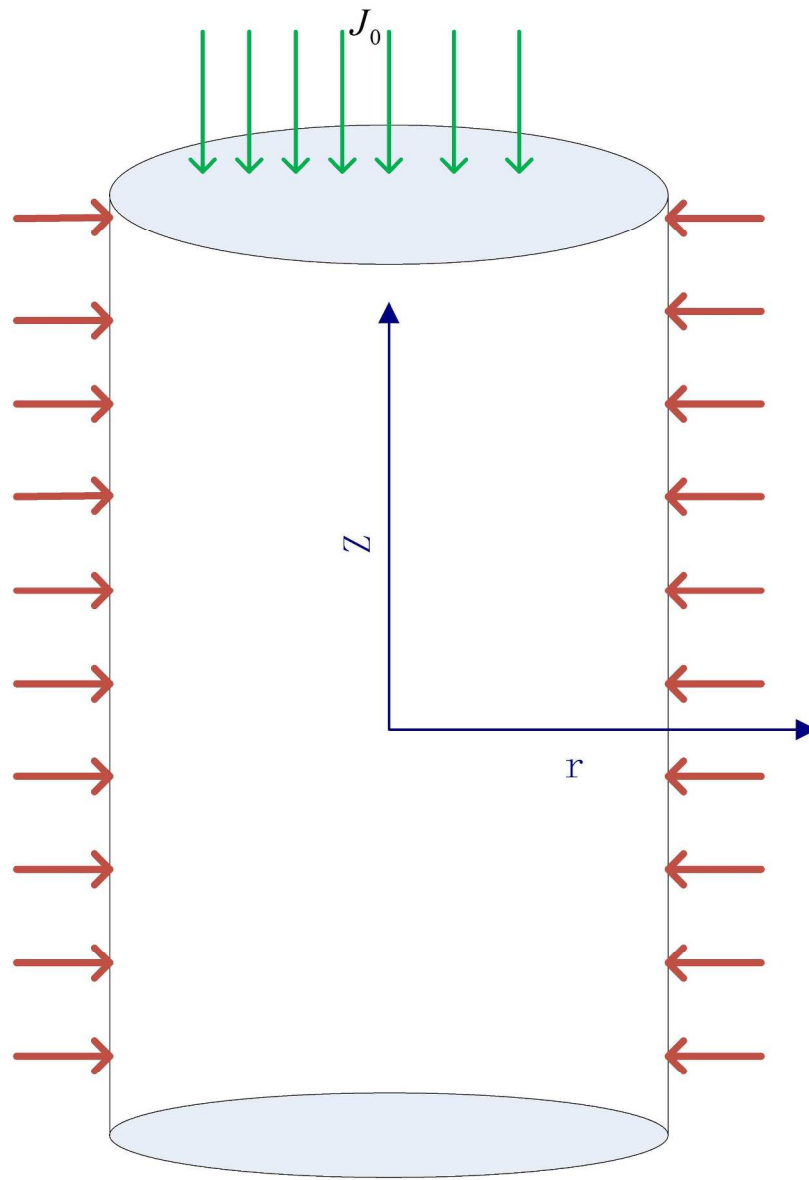
111x157mm (600 x 600 DPI)
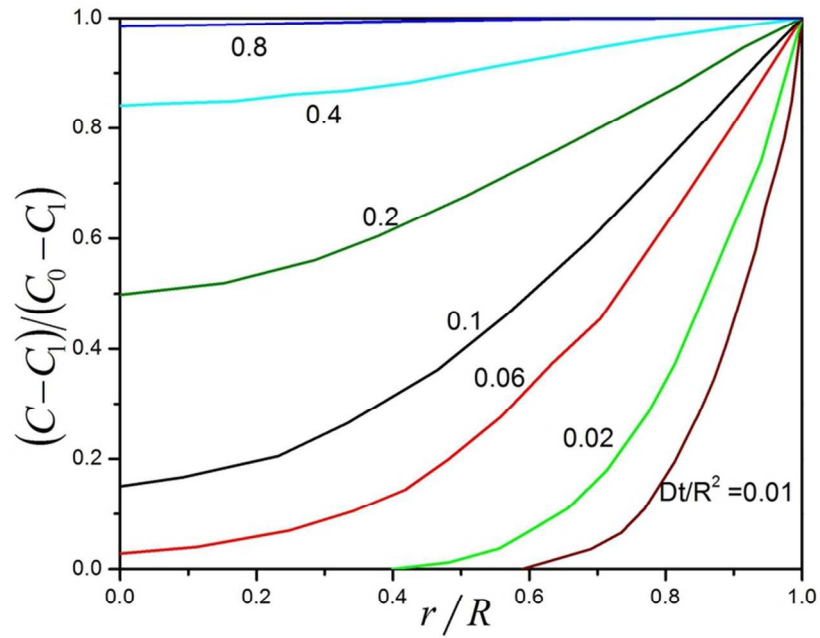
82x63mm (300 x 300 DPI)
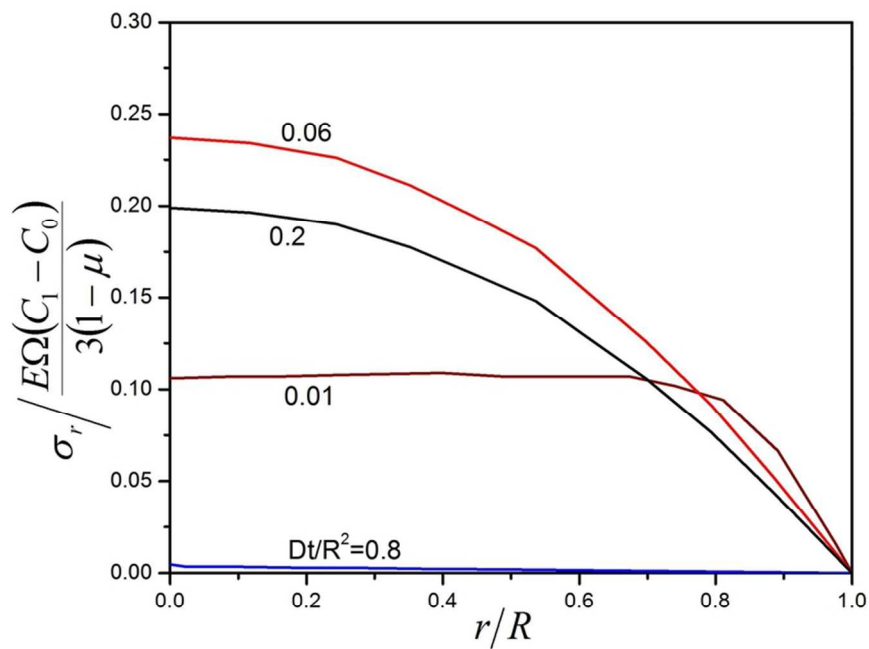
82x63mm (300 x 300 DPI)
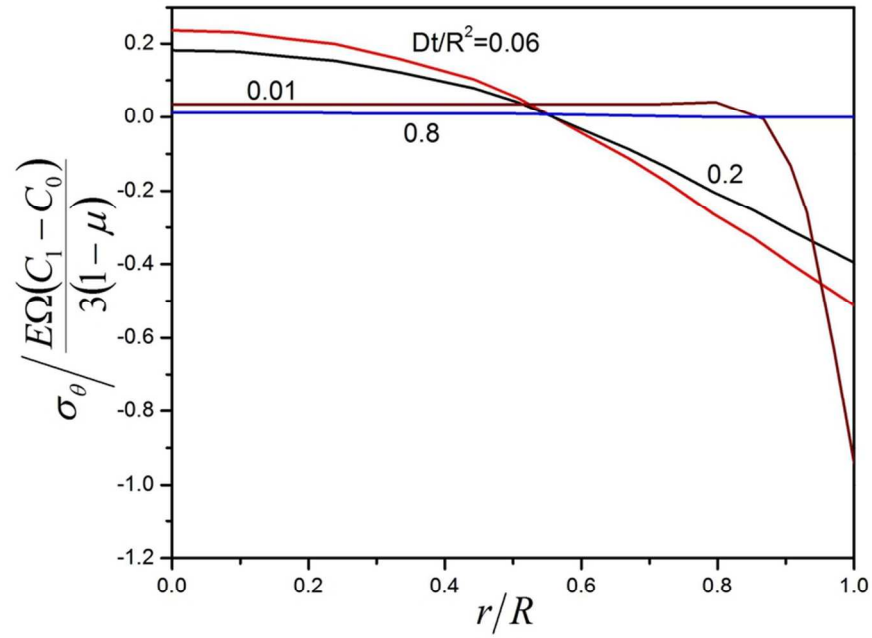
82x63mm (300 x 300 DPI)
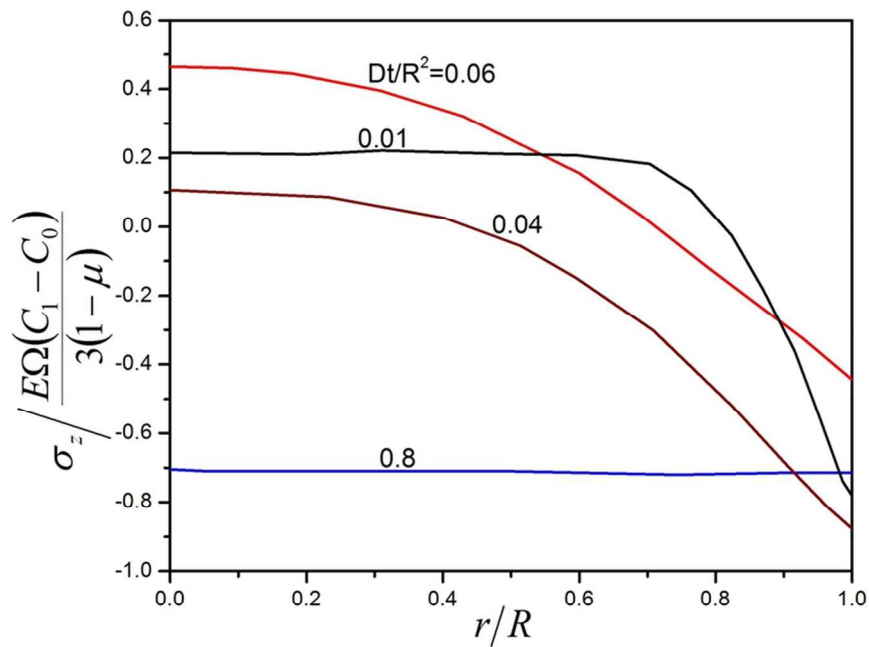
82x63mm (300 x 300 DPI)
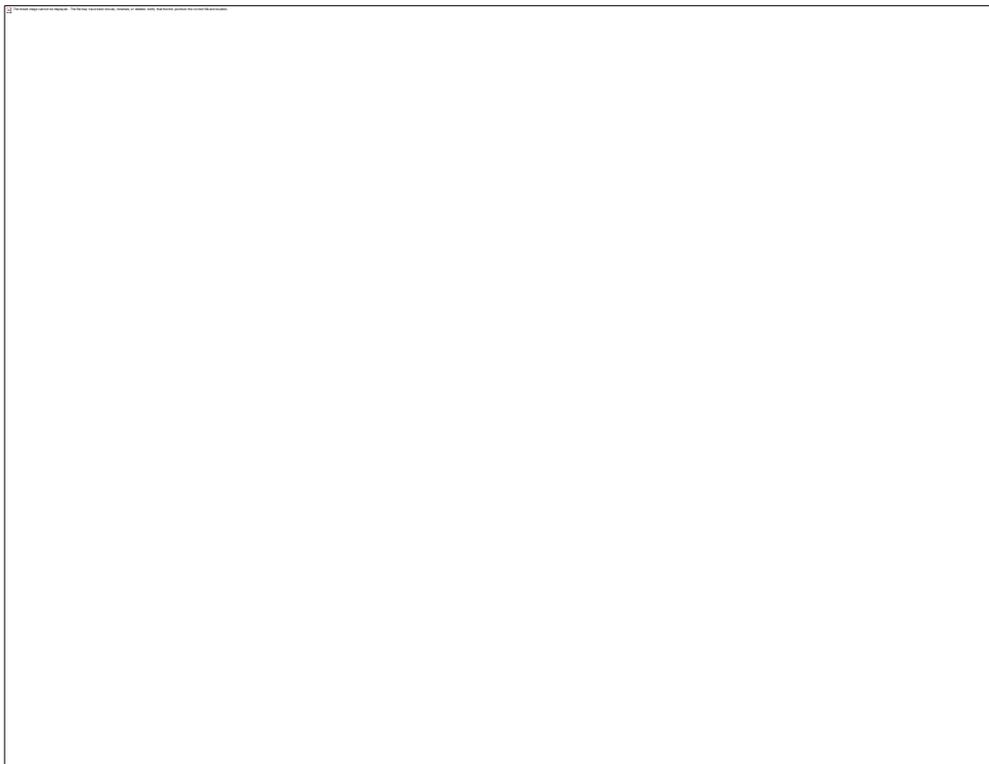
159x122mm (300 x 300 DPI)
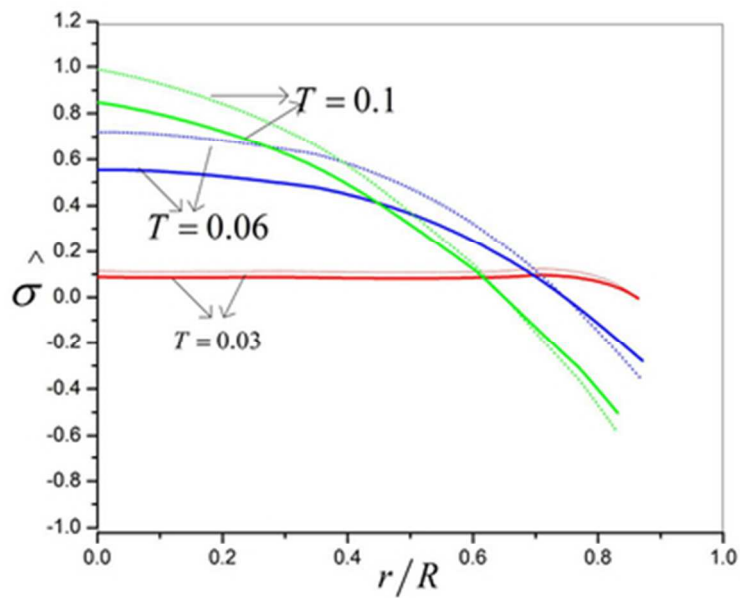
19x14mm (600 x 600 DPI)
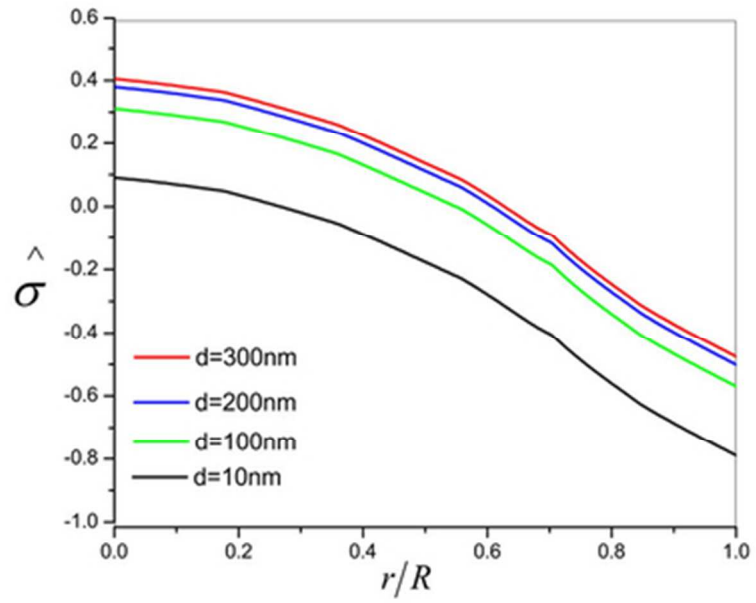
19x15mm (600 x 600 DPI)
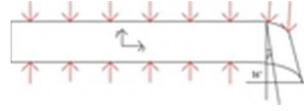
12x4mm (300 x 300 DPI)
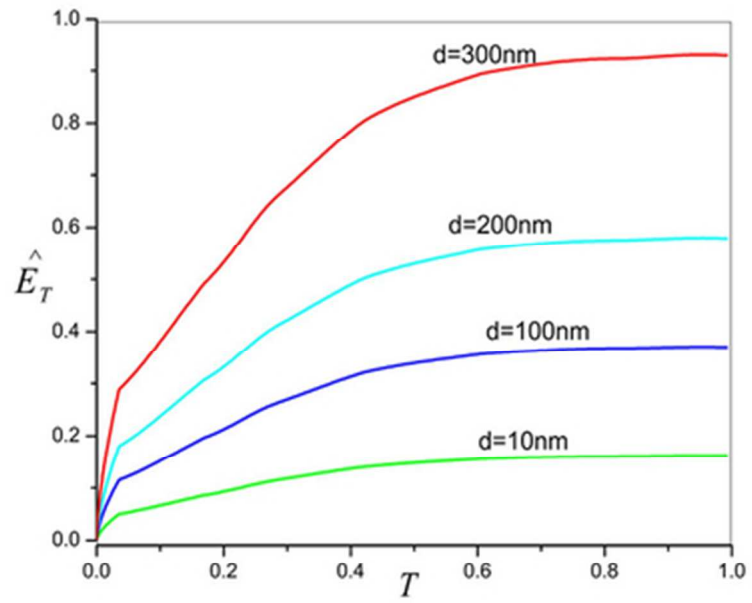
19x15mm (600 x 600 DPI)
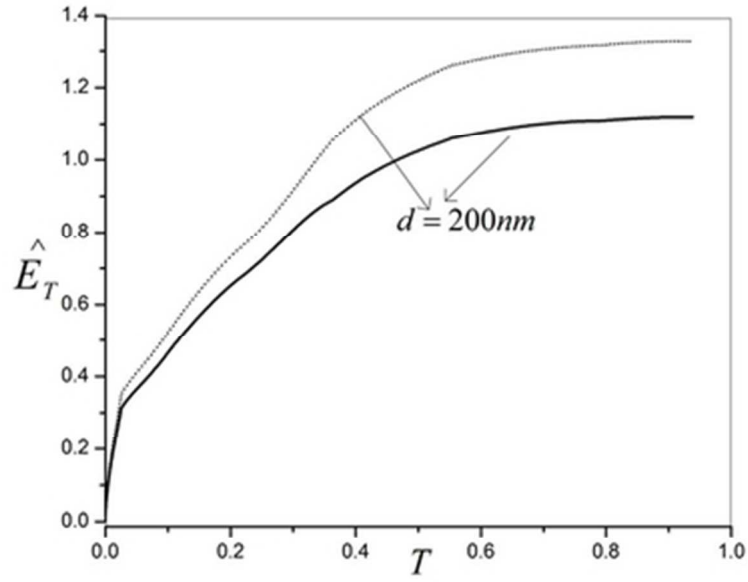
19x14mm (600 x 600 DPI)
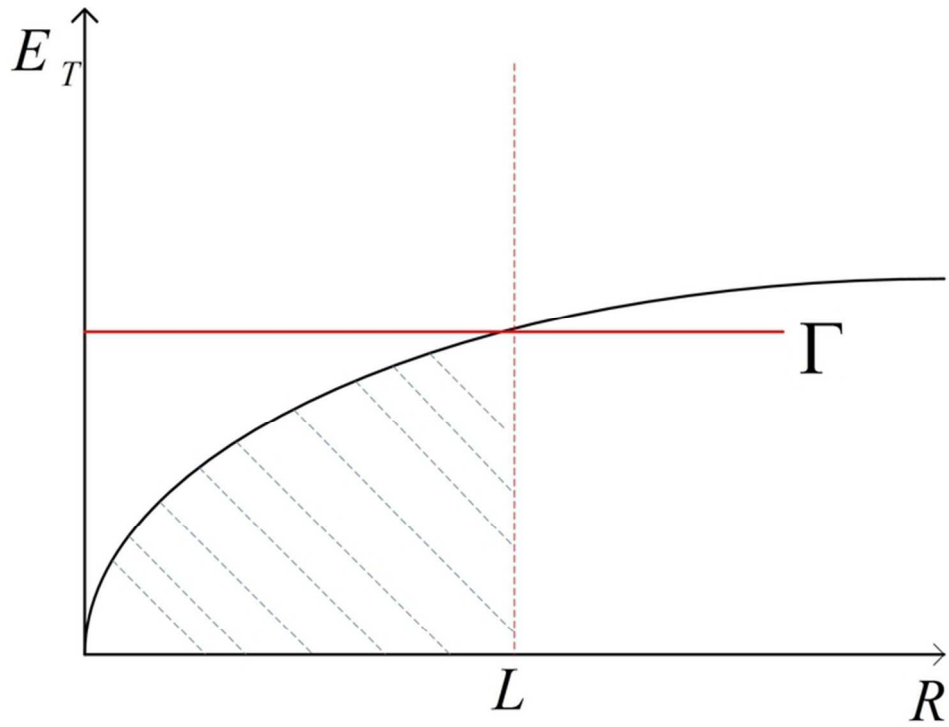
67x48mm (300 x 300 DPI)

131x101mm (600 x 600 DPI)